Facultad de Ciencias
Universidad de La Laguna

Initial reference status of a clinical electron linear accelerator (LINAC).

Vivek Vinod Balani Mahtani

Julio 2019

Supervised by:
Carlos Garrido Bretón
Manuel Eulalio Torres Betancort

79075490H
alu0100966459@ull.edu.es
671 472 373

Contents

Acknowledgements.

I want to start this text by thanking all the professors of the Physics degree, for dedicating their time not only to teach me the fundamentals of science, but also, how my mother likes to say, for "furnishing my head", and not just filling my brain with knowledge, but teaching me how to acquire it.

I couldn't have done this work without my supervisors. I want to thank Professor Carlos Garrido for letting me inside the radiophysics service at the hospital, and for teaching me all that I needed to know to do this work; and Professor Manuel Torres for helping me writing this memory, and for dedicating his time to learn something completely out of his field of knowledge. I also have to thank Ivan, who was a 3^{rd} year resident when I started the project and is now an official radiophysicist working at the *CHUC*, for spending his time on me.

And last, but not least, I want to thank all those people who have, in a way or another, helped me during this 4 years, specially the one person who gave me the idea of studying physics since I was a little child.

Motivation.

En los últimos años se han realizado grandes inversiones en radioterapia, de forma que se han podido adquirir nuevos equipos de tratamiento radiológico para mejorar la terapia con radiaciones en los hospitales. Concretamente, ha llegado un nuevo acelerador lineal al Complejo Hospitalario Universitario de Canarias (CHUC). Sin embargo, antes de poder utilizar estos nuevos equipos, es necesario llevar a cabo una serie de pruebas en ellos, para determinar que funcionan correctamente y no puedan causar perjuicios a los pacientes. Esta es una de las tareas que compete al radiofísico hospitalario. Con este trabajo tengo la oportunidad de acercarme al campo de la radiofísica, y puedo comprobar si realmente es a lo que quiero dedicar mi vida laboral.

Recently, a great invest in radiotherapy has been made, so new equipment has arrived to the *Complejo Hospitalario Universitario de Canarias (CHUC)*. It is necessary to test and check the new systems before they start working with real patients who need to be treated with ionising radiation, because if it doesn't work correctly, it can damage health tissue, which could harm the patient and even cause it's death. This is one of the tasks of radiophysicists, and as I would like to work as one, this final project could approach me to the field, so I can confirm that this is what I want to do after the degree.

List of Figures

List of Tables

Abstract.

Recientemente el desarrollo de la radiofísica y la física médica en España se ha visto apoyado por grandes inversiones, de forma que los hospitales públicos han podido adquirir nuevos equipos para realizar tratamientos. Un acelerador lineal de electrones (LINAC) es un sistema que permite eliminar células cancerígenas mediante haces de fotones (o electrones) con altas energías. En el caso del nuevo acelerador *Truebeam*, estas energías son 6 MV (con y sin filtro aplanador), 10 MV (sin filtro aplanador) y 18 MV (con filtro aplanador).

Los parámetros que se medirán a la hora de determinar el estado de referencia inicial del acelerador se pueden dividir en dos tipos: los relativos a la calidad del haz, definida como sinónimo de la energía del mismo (porcentaje de dosis en profundidad y razón tejido maniquí); y relativos a la dosimetría del campo de radiación (homogeneidad para los perfiles aplanados con filtro, pendiente para los perfiles sin aplanar, y simetría para los dos tipos de perfiles).

Los resultados obtenidos relacionados al haz de 6 MV sin filtro se asemejan considerablemente a los que se reportan en la literatura, comparados debido a que los haces sin filtro son una novedad en el Hospital Universitario. Los resultados de los parámetros en relación al haz con filtro aplanador son coherentes respecto a los valores que se obtienen en los distintos aceleradores del propio Hospital.

Una vez realizadas las medidas, los valores obtenidos se guardarán en el sistema monitor del acelerador, de forma que a la hora de realizar los controles de calidad mensuales, puedan realizarse las comprobaciones necesarias para asegurar que el acelerador funciona correctamente, sin variaciones significativas de estos parámetros característicos de cada una de las energías del haz.

Chapter 1

Introduction.

Abstract. *Las radiaciones ionizantes juegan un papel muy importante en radioterapia y radiodiagnóstico, especialmente en la lucha contra el cáncer. El objetivo principal de la radioterapia es maximizar el control tumoral a la vez que minimizar el daño al tejido sano cercano. Este tipo de tratamiento se lleva a cabo con aceleradores lineales de electrones (LINAC). Se trata de un sistema que permite eliminar células cancerígenas mediante haces de fotones (o electrones) con altas energías. En este capítulo se detalla su historia, sus componentes y su funcionamiento, así como algunas de las características del nuevo LINAC del Hospital Universitario de Canarias.*

Ionising radiations have a very important role in therapy and radio diagnostics of many pathologies, mostly against cancer. In this field, the main purpose of radiation therapy consists in maximising the probability of tumour control, minimising the damage to the healthy tissue. The existing applications and techniques of radiation treatments, have been developed since the advanced technological possibilities introduced in the therapy equipments, the precise parametrization of the radiation-matter interaction processes and the developments in biological effects of radiation on different tissues and organs.

In the last decades, a great number of innovations have been introduced in the equipment and methodology involved in the radiotherapeutic treatment. From the development of new programmes used to delimit the volumes, with the possibility of mixing different types of diagnostic images, to the use of immobilization that reduce the repeatability mistakes in the positioning of patients and new technological developments in the equipments and procedures used in physics dosimetry.

Nonetheless, the fast technological development with the complexity of the newest procedures, carry new challenges and represent new risks. This is why before the clinic implementation of new equipments, an exhaustive revision must be done.

Radiophysicists, who are qualified professionals in everything related to equipments and dosimetry, must be directly involved in the procedures of the acquisition of new equipment, since their technical knowledge and professional criterion are the main factors [1].

1.1. Aim of this work.

This work is meant to determine some of the most relevant parameters which are involved in the periodic review of the LINAC, in order to establish the Initial Reference Status of the '*Truebeam* .

1.2. What is a LINAC?

A linear particle accelerator (LINAC) is a system that accelerates charged subatomic particles or ions to a high speed by subjecting them to a series of oscillating electric potentials along a linear beamline.

LINACs have many applications: they serve as particle injectors for higher-energy accelerators, and are used directly to achieve the highest kinetic energy for light particles (electrons and positrons) in particle physics experiments. But they are also used in medicine, although they generate X-rays and high energy electrons which can conform to a tumour's shape and eliminate cancer cells [1].

1.3. History of LINACs.

The linear accelerator was proposed in 1924 by the Swedish physicist Gustaf Ising, but it wasn't until 1928 when the first LINAC was built, by the Norwegian engineer Rolf Wideröe.This LINAC could accelerate Potasium ions up to 50 KeV.

During the Second World War, very powerful radiofrequency generators were built, needed for the radars. This meant a great development on the design of LINACs, making possible the acceleration of lighter particles such as electrons and protons. In 1946 Luis Álvarez designed an accelerator which measured 875 m length located in a resonant cavity which could accelerate protons up to 32 MeV, based on continuous potentials.

Electron LINACs are different from proton LINACs. The frequencies must be higher in the former ones (to keep up with the fast moving electrons), so the accelerating cavities must be smaller. Development of electron LINACs occurred nearly in parallel in the US (the longest linear accelerator (3.2 km) is located in the SLAC National Accelerator Laboratory, California) and in the UK (Telecommunications Research Establishment—TRE). By November 1946, *Fry et al.*, at TRE, had completed the theoretical design, construction, and testing of a 45cm long, 0.5 MeV LINAC, reported in a 1947 paper. The group kept improving and developing their accelerator. Having achieved 3.5 MeV, by the end of 1948 Fry's group, supported by the British Ministry of Health, started collaborating with the *Radiotherapeutic Research Unit of the British Medical Research Council*, and with the *Metropolitan Electrical Industries* to build an X-ray LINAC for clinical use. An 8 MeV prototype was installed at the Hammersmith Hospital, in London, and the first patient was treated in August 1953. While the 8 MeV was under construction, the Ministry of Health decided to supply some radiotherapy centers in England with 4 MeV LINACs. For this, P. Howard Flanders conceived the design of an isocentric gantry mount for the accelerator in 1949.

This was the beginning of a very successful association between electron LINACs and radiotherapy. Since then, a huge progress has been achieved, both in compactness, reliability, and accuracy [2].

1.4. How does a LINAC work?

In figure 1.1 it is represented a schematic view of a LINAC. Each part is explained in appendix A. Nevertheless, using Figure 1.2 a brief explanation is given for the acceleration structure.

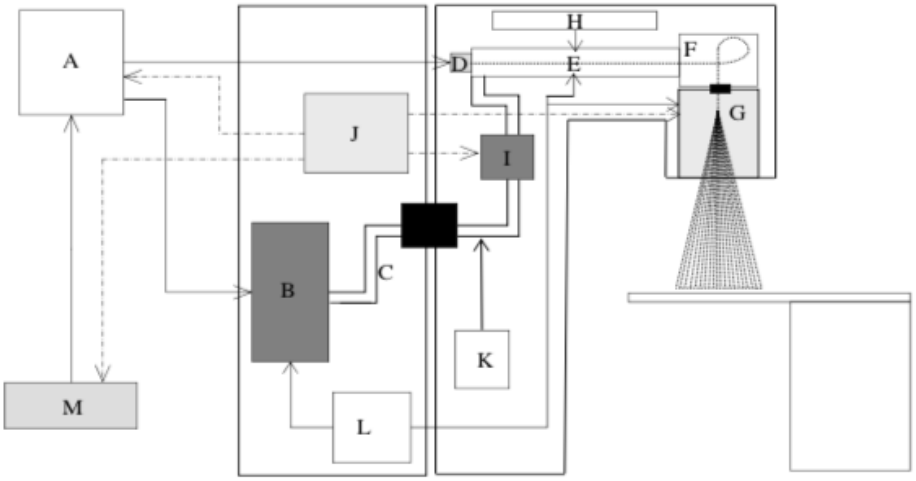

Figure 1.1: Scheme of a LINAC. (A) Modulator. (B) Microwave generator. (C) Wave guide. (D) Electron source and injector. (E) Accelerator guide. (F) Bending magnet. (G) Headboard. (H) Vacuum pump. (I) Frequencies control system. (J) Electric and safety systems. (K) Pressure diffuser. (L) Refrigeration system. (M) Control console [3].

A straight hollow pipe vacuum chamber (H in Figure 1.1) contains the other components of the acceleration structure (E) , and ensures that the accelerated particles won't collide with air molecules.

The particle source (D in Figure 1.1 and S in Figure 1.2) produces the charged particles which the machine accelerates. The design of the source depends on the particle that is being accelerated. For medical purposes electrons are needed and are generated by a cold cathode, a hot cathode, a photocathode, or radio frequency ion sources. The source has its own high voltage supply to inject the particles into the beamline.

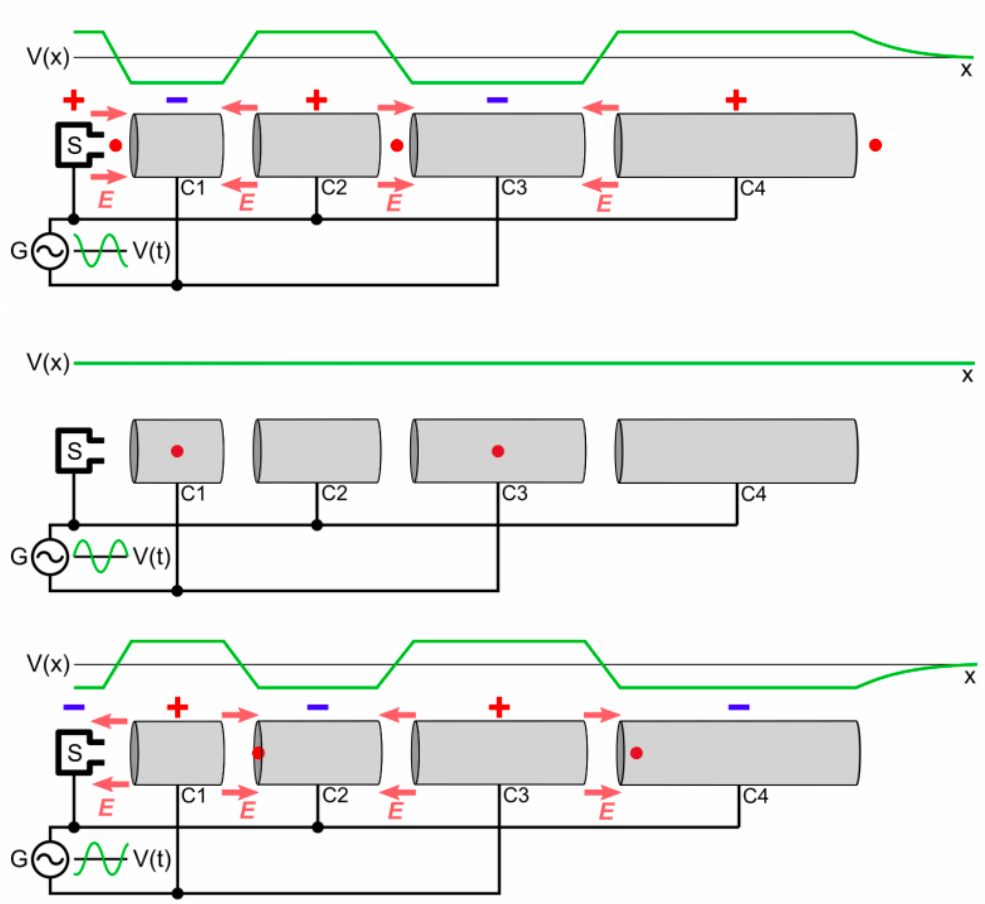

Figure 1.2: Acceleration structure with oscillating potentials.

Extending along the pipe from the source is a series of open-ended cylindrical electrodes (C1, C2, C3, C4 in Figure 1.2), whose length increases progressively with the distance from the source, following the relation:

$$L_n = L_1\sqrt{n} \tag{1.1}$$

where L_1 is the length of the first electrode (C1).

The electrons pass through these electrodes while an electronic oscillator and amplifier (G) generates a radio frequency of AC voltage of thousands of volts and applies it to the electrodes. This is the accelerating voltage that produces the electric field (**E**) which accelerates the particles. As shown, opposite phase voltage is applied to successive electrodes. A high power

accelerator will have a separate amplifier to power each electrode, all synchronized to the same frequency.

A brief demonstration of equation 1.1 is given now:

Assuming that the voltage between the source (S) and the first electrode (C1) is $2V_0$, applying the energy conservation principle, the velocity of the electrons with charge e and mass m_e is given by

$$\frac{1}{2}m_e v_1^2 = 2eV_0 \tag{1.2}$$

and the time in which they go through the first electrode is $t_1 = L_1/v_1$. With this, the following relation is obtained

$$t_1 = \frac{L_1}{2}\sqrt{\frac{m_e}{eV_0}} \tag{1.3}$$

When the electrons go through the first electrode to the second, the potential has changed its polarity, so the particles are accelerated with an additional energy of $2eV_0$. The velocity and time then will be:

$$\frac{1}{2}m_e v_2^2 = 4qV_0 \quad ; \quad t_2 = \frac{L_2}{v_2} = \frac{L_2}{2}\sqrt{\frac{m_e}{2eV_0}} \tag{1.4}$$

As t_1 needs to be equal to t_2, it is obtained that $L_2 = L_1\sqrt{2}$. By doing the same between the second and the third electrode, where the additional energy is $6eV_0$, it is proved that $L_3 = L_1\sqrt{3}$. So in the $n-th$ electrode, as the energy increases as $E_n = n2eV_0$, the length of each electrode satisfies the relation 1.1.

At the end of the acceleration structure, there is a target (located in the Headboard in Figure 1.1) with which the particles collide. If electrons are accelerated to produce X-rays then a water cooled tungsten target is used. Behind the target are various detectors for the particles resulting from the collision of the incoming particles with the atoms of the target. These X-rays have the same energy as the accelerated electrons, since the radiation is created by the breaking of the electrons (*bremsstrahlung*) [1, 4].

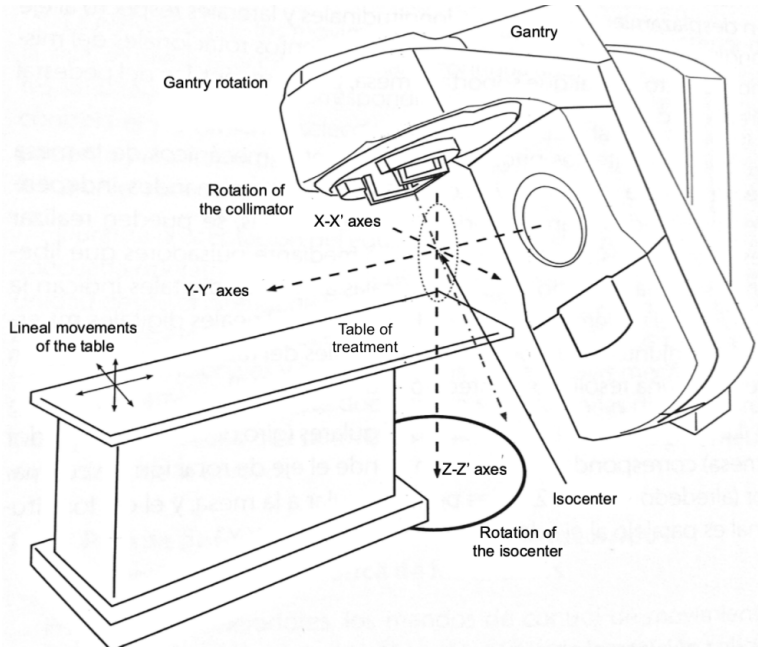

Figure 1.3: Degrees of freedom of a LINAC [1].

In figure 1.3 it is shown a schematic view of a LINAC and its possible movements. A perfect alignment of the radiation field with the region of the patient in treatment is required for an efficient and accurate use of the equipment. The assembly of the unit ensures the reproducibility of the mechanical movements, accomplished because of the mechanical stability of the equipment and the sequence of movements.

The gantry rotation system (around the Y-Y' axis) it is usually servo-controlled, this is, the rotation speed varies continuously under manual control, while in dynamic techniques this speed is precisely controlled and proportional to the absorbed dose rate, ensuring that the given dose per angular unit is constant.

1.5. The new LINAC: 'Truebeam ".

There are some enterprises which develop medical LINACs. One of them is named *Varian Medical Systems*. They have been producing tools that harness the power of X-ray energy to benefit humankind since the 1950. Their history is one of pioneering developments in the fields of radiotherapy,

radiosurgery, X-ray tube technology, digital image detectors, cargo screening, and non-destructive testing. Today, they have a robust product portfolio and long-standing relationships with many of the world's leading clinicians. As *Varian* continues to grow, their staff of approximately 6.500 employees in 70 sales and support offices around the globe is developing innovative, cost-effective solutions that help make the world a healthier place [5].

In Figure 1.4 it is shown the new Varian LINAC bought by the *CHUC*, the *Truebeam* .

Figure 1.4: "Varian Truebeam "

It can produce 2 photon energies, 6 MV[1] and 18 MV, with a flattening filter (FF), and 2 photon energies without the flattering filter (FFF, Flattening Filter Free), 6 MV and 10 MV. The energies without filter are a novelty at *CHUC*, because all of the 3 previous LINACs have a fixed flattering filter. Treatments without filter allow a shortening of the exposure time, though they provide more dose. This work only focuses on the energy of 6 MV with and without the flattening filter.

[1]Mega Volts are not an energy unit, but it is used as a reference for photon beams created by the same MeV electrons.

Chapter 2

Initial reference status.

Abstract. *Tras el proceso de aceptación del nuevo equipo, éste ha de someterse a una serie de pruebas para determinar el estado inicial de los parámetros que servirán para el correcto mantenimiento del acelerador.*

La caracterización de un haz de radiación implica conocer la distribución de dosis tridimensional sobre el volumen irradiado. La variación volumétrica de dosis absorbida se obtendrá a partir de las curvas de dosis absorbida en profundidad y de los perfiles de dosis medidos para distintos tamaños de campo y profundidades. En este capítulo se explican con detalle algunos de los parámetros más relevantes a la hora de determinar este estado de referencia para el nuevo "Truebeam" de Varian.

Once the new equipment has been accepted by the responsible of the quality program, the initial reference status of the LINAC has to be established, according to the acceptance tests. This will allow the periodic check out of the equipment along it's useful life.

The description of a clinical radiation beam implies the knowledge of the three-dimensional distribution of the dose on the radiated volume. The volumetric variation of the absorbed dose will be determined by the curves

of depth-dose, measured along the central axis and by the measured dose profiles for different field sizes and depths.

It is important to distinguish between the parameters of the flattened and unflattened profiles. Nevertheless, the differences between FFF and FF in terms of quality assurance is mainly related to beam dosimetry, and not to mechanical characteristics of the linear accelerator, for which the standard quality assurance procedures still hold. It is clearly not necessary to introduce any modification to a consolidated quality assurance process for nondosimetric checks [6].

In this work only the most relevant parameters will be studied: some referred to the quality of the radiation beam (absolute dose in water and percentage depth-dose) and some referred to the characterization of the radiation field (homogeneity for FF, slopes for FFF and symmetry of both of the profiles).

2.1. Quality of the radiation beam.

The term *quality of the beam* is used as a synonym of the energy of the beam. There are some parameters that describe the quality of the beam. All of them are based on the penetration of the beam in a continuous and homogeneous system, like water [1].

2.1.1. Percentage Depth-Dose (PDD).

The percentage Depth-Dose is defined as the percentage of absorbed dose at a depth (z) in the central axis, normalized to the dose at a reference depth (z_r) in the mentioned axis, at a constant at a constant source-surface distance (SSD) and field size. It is usual to establish the reference depth at the maximum absorbed dose (d_{max}) [1]:

$$PDD = \frac{D_z}{D_{zr}} \cdot 100(\%) \tag{2.1}$$

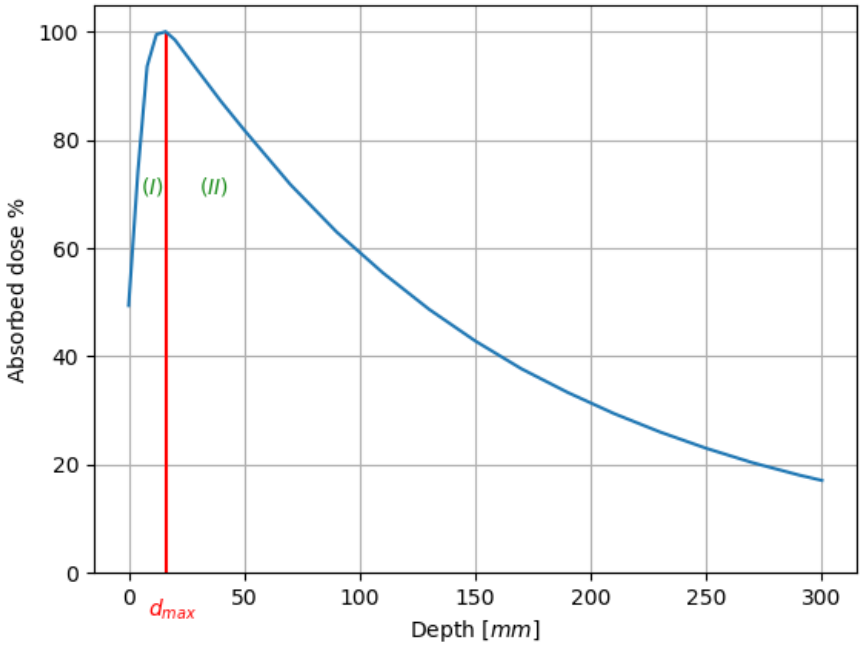

Figure 2.1: PDD curve obtained with a 6 MV beam.

In Figure 2.1 it is shown the PDD curve of a 6 MV beam. Two regions can be clearly distinguished. First, a *build-up* zone (I), between the surface and d_{max}. It has a growing form because of the initial increase of secondary electrons, generated as the result of the interaction of the photons with the system. These electrons have a scope of approximately d_{max}. Afterwards, the curve is decreasing in an exponential form (II), which determines the quality of the photon beam, and it's because of the reduction of the photon fluence with depth, caused by the attenuation of photons in the system.

2.1.2. Tissue-Phantom Ratio (TPR).

It is defined as the absorbed dose in water at a depth (z) of the central axis, normalized to a reference depth (z_r), keeping constant the Source-Detector distance (SDD) and the field size in the detector's plane.

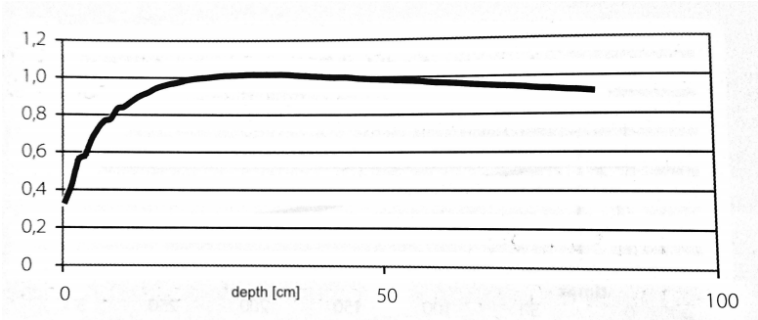

Figure 2.2: Tissue-Phantom Ratio curve [1].

In Figure 2.2 it is shown a TPR curve normalized to the maximum absorbed dose.

2.1.3. Parameters of the quality of the beam.

Without the previous definitions it's not possible to describe the quality of the beam. The main parameters are:

$\mathbf{TPR_{20,10}}$: It is the most used parameter, defined as the relation of the absorbed dose at 20 and 10 cm depth, keeping constant the $SDD = 10$ cm and a 10×10 cm^2 field size in the detector's plane.

$\mathbf{PDD_{20,10}}$: It is defined as the relation of the absorbed dose at 20 cm and 10 cm depth, keeping constant the Source-Surface Distance ($SSD = 100$ cm) and at a field size of 10×10 cm^2. It is easier to measure this parameter than the $TPR_{20,10}$, and they can be related with [1]:

$$TPR_{20,10} = 1.2661 PDD_{20,10} - 0.0595 \tag{2.2}$$

2.2. Absolute reference dose.

The absorbed dose is equal to the absorbed energy divided by unit of mass in a material in which the radiation goes through. It is given in Rad or $Gray$ (GY) ($1Gy = 1J/kg$). The energy is invested in the production

of electric charges by ionisation. This occurs by 3 mechanisms: compton scattering, photoelectric effect and pair production.

The absolute dosimetry determines the absorbed dose at a reference point in Grays. The reference dose is measured in a $10 \times 10\ cm^2$ field at a source-surface distance (SSD) of 100 cm and at a depth of 10 cm.

It is important to define the Monitor Unit (MU) as a certain quantity of charge (ionisation charge) collected by the monitor cameras which are inside the headboard. Each quantity of MU equals a shooting time of the LINAC [1, 7].

The absorbed dose in water, at the reference depth (z_{ref}) for a reference beam with a quality Q is given by:

$$D_{w,Q} = M_Q N_{D,w,Q_0} k_{Q,Q_0} \tag{2.3}$$

where M_Q is the measurement of the dosimeter corrected by the $F(T,P)$ factor, N_{D,w,Q_0} is the calibration factor of the dosimeter in terms of absorbed dose in water, obtained from the calibration laboratory[1], and k_{Q,Q_0} is the correction due to the effects of the difference between the reference quality Q_0 and the real quality measured Q. This factor is defined as the relation of the calibration factors of the ionisation chamber between the qualities Q and Q_0:

$$k_{Q,Q_0} = \frac{N_{D,w,Q}}{N_{D,w,Q_0}} \tag{2.4}$$

The most used reference quality for the calibration of ionisation chambers is the gamma radiation of ^{60}Co [7].

2.3. Dosimetric characterization of the radiation field.

The dosimetric characterization of the radiation field delimited by the collimation system is performed with the dosimetric study of the absorbed dose profiles obtained at the different recommended depths. The analysis of

[1] It is given in the manual of the ionisation chamber.

these profiles allows the determination of some relevant and specific geometric and dosimetric parameters, according to the design of the headboard, the size of the field, the quality of the beam and the measure depth [1].

In Figure 2.3 it's shown an example of the profiles for the same field size with and without filter.

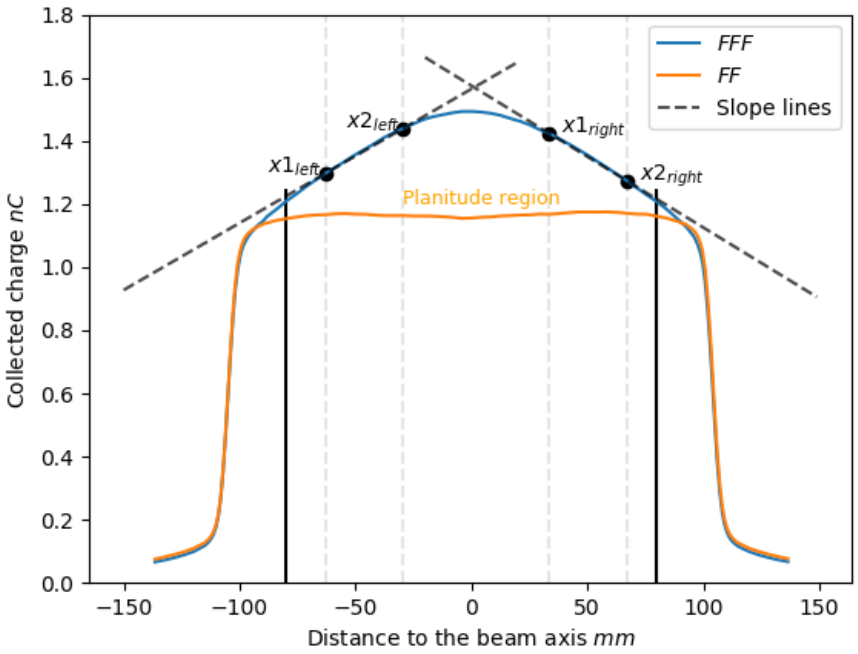

Figure 2.3: Differences between unflattered and flattered profiles for a $20 \times 20\ cm^2$ field.

As FFF beams deliver higher dose to the central axis (as no flattening filter attenuates the beam), FFF and FF beams should be mutually renormalized to superimpose the profile fall-off (field edge). Two methods can be followed: the inflection point or the renormalization value, but in this work will only be obtained the renormalization value as follows [6]:

$$Renorm = \frac{a + b \cdot FS + c \cdot depth}{1 + d \cdot FS + e \cdot depth} \tag{2.5}$$

where FS is the field side in cm, depth is the measuring depth in cm, and a, b, c, d, e are the fitting parameters. In table 2.1 this parameters are reported

for the *Truebeam*. The renormalization factor is applied to the FFF beams after the corresponding FF beams are normalised to the maximum dose (100%).

a	b (cm^{-1})	c (cm^{-1})	d (cm^{-1})	e (cm^{-1})
91.3	1.20	1.38	-0.0075	0.014

Table 2.1: Fitting parameters [11].

2.3.1. Homogeneity of the FF profiles.

It is a dosimetry parameter which allows to assess the flatness of the dose profiles. It is defined as the maximum percentage variation in relation to the absorbed dose inside the homogeneity region, which is delimited by the 80% of the radiation field size (planitude region in Figure 2.3).

The distribution of the energy fluency in photon beams is not uniform, though it is higher along the main axis than in the borders. To homogenise the absorbed dose distribution along the radiation field, a flatting filter (cone shaped) is located across the beam, of a thickness and material depending on the energy of the beam.

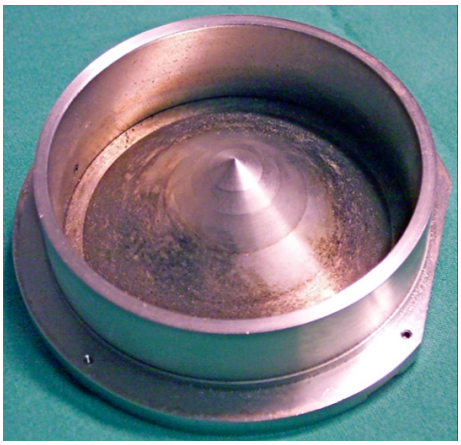

Figure 2.4: A conventional flattening filter [8].

In Figure 2.4 it is shown a flattening filter of a clinical LINAC. Its thoughtful design and calibration, with the precise beam alignment, would allow the energy fluency rate to be quite uniform along the radiation field. The filter

is designed in a way that it's thickness decreases from the middle to the borders, which disturbs the spectrum of the X-rays and so, the quality of the beam along the radiation field, giving as a result a lower mean energy of the beam at the periphery of the beam than at it's central area. The contribution of the scattered radiation increases with depth. These disturbances in the quality of the beam, carry important changes in the homogeneity of the profiles as functions of depth.

The homogeneity is given by the following relation [1]:

$$H(\%) = \frac{D_{max} - D_{min}}{D_{max} + D_{min}} \times 100(\%) \tag{2.6}$$

where D_{max} is the maximum absorbed dose and D_{min} is the minimum absorbed dose.

2.3.2. Slopes of the FFF profiles.

The peak shape of the FFF profile can be defined by the "slope" parameter describing the left and right inclinations of the profiles. Because the FFF profile depends on the energy, with different shapes in terms of concavity or convexity of the slopes, a more general definition for a gradient of the two sides of the profile needs to be defined. This parameter can be the slope of the line passing through two fixed points on the profiles located at 1/3 and 2/3 of the half beam (defined by the field size), according to:

$$Slope = \frac{D(x_1) - D(x_2)}{x_1 - x_2} \tag{2.7}$$

where $D(x_1)$ and $D(x_2)$ are the absorbed doses at x_1 and x_2 (see Figure 2.3), which are defined as a function of the size of the field:

$$x_1 = \frac{Size}{2} \cdot \frac{1}{3} \; ; \; x_2 = \frac{Size}{2} \cdot \frac{2}{3} \tag{2.8}$$

for the right side of the profile; and for the left side:

$$x_1 = -\frac{Size}{2} \cdot \frac{2}{3} \; ; \; x_2 = \frac{Size}{2} \cdot \frac{1}{3} \tag{2.9}$$

The slope parameter has two aims: on one side it assures that the beam is symmetric around the collimator axis (together with the symmetry parameter) by checking its value along the main axes; on the other side its value assures the correctness of the beam energy (similarly to the beam quality parameters, even if in an indirect way) [6].

2.3.3. Symmetry of the dose profiles.

The symmetry of the dose profiles, measured along the radiation field, is a dosimetric parameter which allows to evaluate the equivalence on the distribution of the absorbed dose in symmetrical points about the main axis in both sides of the profile.

The study of the degree of symmetry in the dose distribution obtained in the profiles, allows the correct alignment and positioning of the different parts of the headboard about the axis of the beam. In X-rays the center of the spotlight must be perfectly aligned with the flattening filter, and the colimation system will describe an arc centered about the spotlight.

On the one hand, the symmetry of the flattened profiles is defined as the maximum percentage variation of the absorbed dose in symetrical points inside the homogeneity region, and it is given by [1]:

$$S(\%) = max\left(\frac{D_x}{D_{-x}}\right) \times 100(\%) \tag{2.10}$$

where D_x is the absorbed dose at the positive side of the axis of measurement and D_{-x} is the absorbed dose at the negative side. This means that the symmetry will be determined by the points where the reason D_x/D_{-x} is further than the unit.

On the other hand, the symmetry of the not flattened profiles is given by the maximum variation of the absorbed dose in symmetrical points between the central axis:

$$S = max(D_x - D_{-x}) \tag{2.11}$$

Chapter 3

Materials and methods.

Abstract. *En este capítulo se realiza una explicación detallada de los diferentes elementos necesarios para llevar a cabo las medidas. Se explica también el procedimiento seguido a la hora de determinar los diferentes parámetros explicados en el capítulo anterior. Todos ellos se miden en un medio continuo y homogéneo, el agua.*

In this chapter, a detailed explanation of the material needed for the measurements is given. It is also explained the procedure of how the measurements and data are obtained, in order to establish the previously defined parameters. All of the measurements are made inside a continuous and homogeneous material, water.

3.1. Equipment.

For the different measurements, the following equipment is needed:

- Ionisation chambers (Figure 3.1). These detectors are based on the measurement of the ionisation produced by the radiation in the gas,

which is inside its volume [9]. In the measurements two chambers were used. For the absolute dose, a cylindrical shaped chamber with a volume of 0.6 cm^3, which collects more charge, so it has better resolution; and for the relative dosimetry, a 0.125 cm^3 "pinpoint" chamber, which is smaller, so it has less ionisation but more spacial resolution.

As mentioned before, the required value for Equation 2.3, N_{D,w,Q_0}, is obtained from the manual of the chamber, and is equal to 5.447 cGy/nC in this case.

These chambers are opened to air, this means that the thermodynamic variables of the air inside the chamber depend on the outside conditions, which implies that the chamber must be calibrated to these values:

$$F(P,T) = 2.5921\ mmHg/K\ \times \frac{(273.2+T)}{P} \tag{3.1}$$

Figure 3.1: Ionisation chamber.

The day of the measurements the value of the calibration parameter was $F(735.7\ mmHg, 17.36°C) = 1.024$.

- Electrometer (Figure 3.2). The ionisation chambers are connected to a control unit that chooses the voltage and an electrometer which allows to read the amount of produced charge (in nC). The ionisation current

is very small, so the pack of the electrometer with the chamber acts as an operational amplifier.

Figure 3.2: Electrometer

- Water tank (Figure 3.3). It is a $600 \times 500 \times 408$ mm^3 container filled with distilled water. It's opened in its upper face, and inside there is located an ionisation chamber, in a rail system which allows to collect measurements along the 3 dimensions.

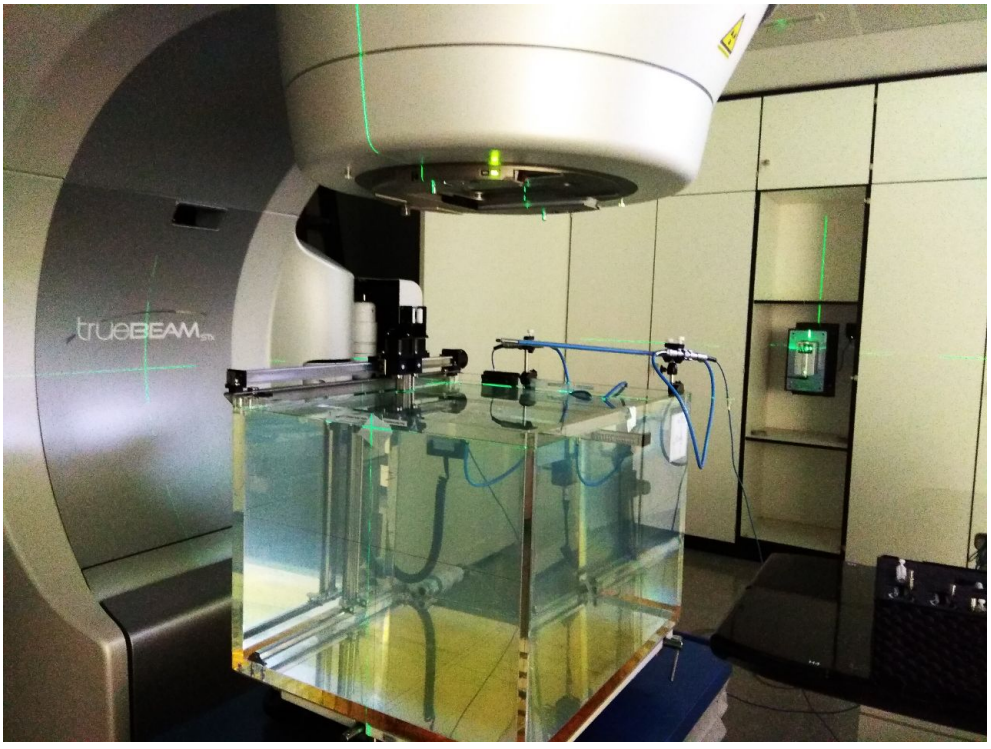

Figure 3.3: Water tank.

3.2. Data gathering.

As explained in the previous section, all of the measurements were made in the water tank. The difference between them is the movement of the ionisation chamber. For the parameters which characterise the beam, the chamber moves from the bottom of the tank to the surface. It can be done from top to bottom, but as the first point is exactly the surface, if the movement starts from it, the braking of the surface could carry more uncertainty in the measurements.

On the other hand, the characterisation of the field is accomplished by moving the chamber at a fixed depth from side to side, along the x-axis (crossplane) and the y-axis (inplane).

3.2.1. Quality of the beam.

To determine the parameters which define the quality of the beam, the PDD curves were obtained, by moving the ionisation chamber from bottom to top inside the water tank. The ionisation chamber was programmed to acquire more data inside the "build-up" region and right after d_{max}, where the curve is not as smooth as while decreasing (every 4 mm from the surface until 20 mm and every 10 mm until 300 mm). Then, with equation 2.2 the value of the $TPR_{20,10}$ is obtained.

3.2.2. Absolute reference dose.

$\text{TPR}_{20,10}$	0.59	0.62	0.65	0.68	0.7
k_{Q,Q_0}	0.999	0.997	0.994	0.99	0.988

Table 3.1: Extract from table 14 of [10].

The values for the correction factor k_{Q,Q_0} are obtained from the $TPR_{20,10}$ using the values of table 3.1, extracted from the protocol [10] using the following formula:

$$k_{Q,Q_0} = (k_{(Q,Q_0)+} - k_{(Q,Q_0)-}) \times \frac{TPR_{20,10} - TPR_{(20,10)-}}{TPR_{(20,10)+} - TPR_{(20,10)-}} + k_{(Q,Q_0)-} \quad (3.2)$$

where $TPR_{20,10}$ is the measured quantity using Equation 2.2, $TPR_{(20,10)-}$ is the nearest lower value from the table, $TPR_{(20,10)+}$ is the nearest higher value from the table, and $k_{(Q,Q_0)-}$ and $k_{(Q,Q_0)+}$ are its corresponding quality factors from the table.

After getting this parameter, using equation 2.3 the Absorbed Dose in water can be obtained.

3.2.3. Dosimetric characterization of the radiation field.

To determine the parameters which characterise the radiation field, the profiles along the crossplane and inplane axes at different depths had to be obtained. This is achieved by irradiating the water tank with beams of different field sizes and moving the ionisation chamber from side to side. As mentioned before, the ionisation chamber collects more data in the regions where the profiles are less smooth, such as the penumbra[1] and the *shoulders* of the profiles. Then, with equations 2.6, 2.7, 2.10 and 2.11 the values for the homogeneity, slopes and symmetry are obtained.

[1]Penumbra is defined as the distance between the 80% and the 20% of the absorbed dose.

Chapter 4

Results and discussion.

Abstract. *En este capítulo se presentan los datos obtenidos experimentalmente en el Truebeam . Los valores de los diferentes parámetros se guardarán en la base de datos del sistema controlador del acelerador para revisar en el control de calidad mensual que no hay variaciones significativas en ellos.*

In this chapter the obtained results in the *Truebeam* for the previously defined parameters are shown. This values will be saved in the database of the LINAC system to review every month, in the quality control, that there are not significant changes in them, so radiophysicist can assure that the LINAC is working as it should and won't cause any harm to the patients in treatment.

4.1. PDD.

In the first place, to determine the quality of the beam, the PDDs are required. In Figure 4.1 are shown different PDD curves for different field sizes, as well as each depth of maximum absorbed dose (d_{max}) in Table 4.1.

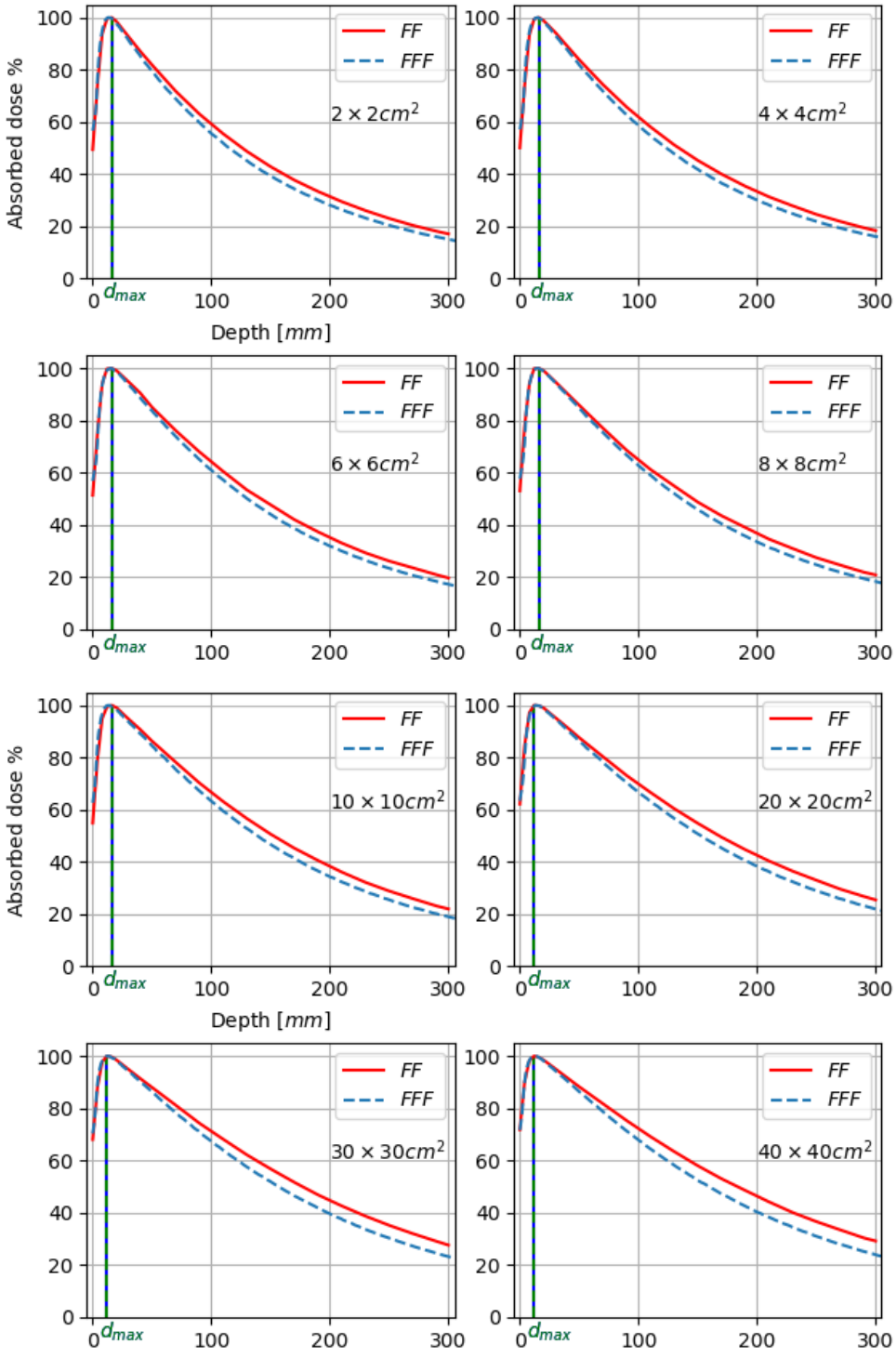

Figure 4.1: 6 *MV FF* PDD curves for different field sizes.

Field size $[cm^2]$	d_{max} $[mm]$	
	FF	FFF
2×2	16.00	13.00
4×4	16.00	15.00
6×6	16.00	15.00
8×8	16.00	15.00
10×10	16.00	14.00
20×20	12.00	13.00
30×30	12.00	12.00
40×40	12.00	13.00

Table 4.1: Depths of the maximum absorbed dose in Figures 4.1

Comparing the flattened and the unflattened PDDs (Figure 4.1 and Table 4.1), it is seen that the absorbed dose at the surface in the flattened beams is lower than in the unflattened beams. This is due to the fact that in the unflattened beam there is more scattered radiation. It can also be seen that the unflattened beams decay faster than the flattened beams. The depth where the maximum absorbed dose is reached is lower in the FFF beams because the scattered radiation has a bigger contribution to the main axis in the unflattened beams.

4.2. Quality of the beam.

With the values of the PDD in the reference field (10×10 cm^2), the TPR is calculated using formula 2.2, and afterwards, the value of k_{Q,Q_0} is obtained by using Equation 3.2.

Beam	D_{10} (%)	D_{20} (%)	$PDD_{20,10}$	$TPR_{20,10}$	k_{Q,Q_0}
6 MV FF	66.92	38.19	0.571	0.663	0.9923
6 MV FFF	63.25	34.3	0.542	0.627	0.9963

Table 4.2: Quality factor for the ionisation chamber.

The obtained results for the $TPR_{20,10}$ values are similar to the results obtained in [11] (Table V) and in [6] (TableV), which were also studied in a $Truebeam$ LINAC.

The FFF beam quality is lower than the corresponding FF quality, even though they have the same nominal energy. This can be explained due to the fact that, although the photon beam energy spectrum generated at the target is the same for FF and FFF modes, there is a greater beam hardening caused by the presence of the flattening filter in the standard beams [11].

4.3. Absolute Reference Dose.

Using the quality factor obtained in the previous section, equation 2.3 can be applied to get the absolute reference dose, at a 10×10 cm^2 field and at 10 cm depth. In table 4.3 this results are presented.

Beam	$N_{D,w,Q}$ $[cGy/nC]$	M_Q $[nC]$	$D_{w,Q}$ $[cGy]$
6 MV FF	5.405	12.87	69.6
6 MV FFF	5.427	12.32	66.8

Table 4.3: Absolute reference dose using Equation 2.3 and k_{Q,Q_0} in Table 4.2.

4.4. Dose profiles.

4.4.1. FF beams.

In Figures 4.2 and 4.3 are represented the obtained profiles for different field sizes and depths for the FF beam. In Tables 4.4, and 4.5 the results of the homogeneity and symmetry are shown for the represented fields.

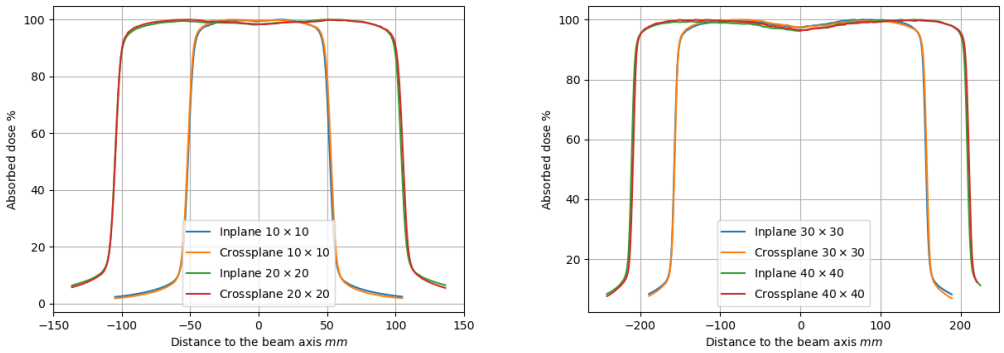

Figure 4.2: Profiles at 5 *cm* depth for FF beam.

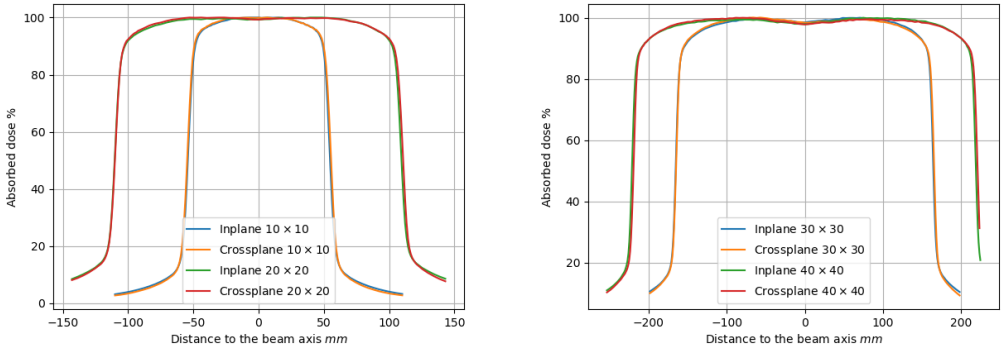

Figure 4.3: Profiles at 10 *cm* depth for FF beam.

Size $[cm^2]$	Homogeneity (%)		Symmetry (%)	
	Crossplane	Inplane	Crossplane	Inplane
10×10	1.14	1.32	101.88	102.31
20×20	0.83	0.92	100.69	101.12
30×30	1.30	1.33	101.70	102.13
40×40	1.78	1.91	103.08	103.66

Table 4.4: Homogeneity and symmetry for FF profiles at 5 *cm* depth.

Size $[cm^2]$	Homogeneity (%)		Symmetry (%)	
	Crossplane	Inplane	Crossplane	Inplane
10×10	1.64	1.75	103.03	103.42
20×20	1.08	1.41	101.65	102.26
30×30	1.29	1.38	100.57	101.42
40×40	1.12	1.15	100.46	101.19

Table 4.5: Homogeneity and symmetry for FF profiles at 10 *cm* depth.

It is noticed by comparing the form of the profiles at the different depths that the flattening filter is calibrated to 10 *cm*. The central part of the profiles at 5 *cm* depth it's lower than the central part of the 10 *cm* depth profiles, due to the fact that the flattening filter assures that the homogeneity of the profiles at 10 *cm* depth is nearer to one than other depths.

4.4.2. FFF beams.

In Figures 4.4 and 4.5 are presented the obtained profiles (normalized to the maximum absorbed dose in the central axis). In Tables 4.6, 4.7 and 4.8 the obtained results of symmetry and slopes are reported.

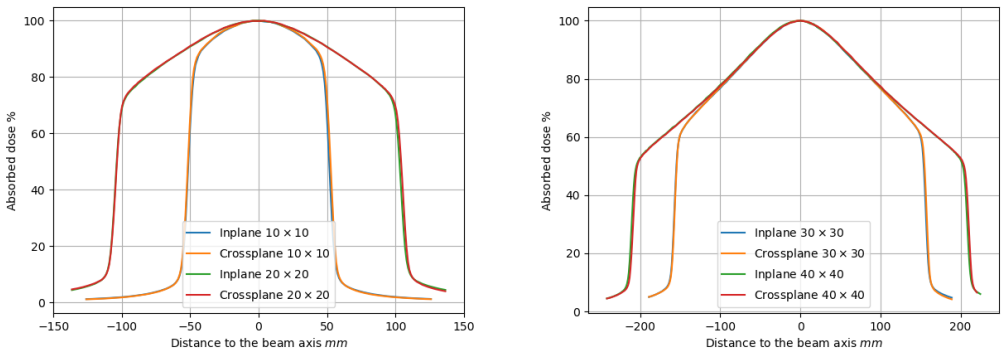

Figure 4.4: Profiles at 5 *cm* depth for FFF beam.

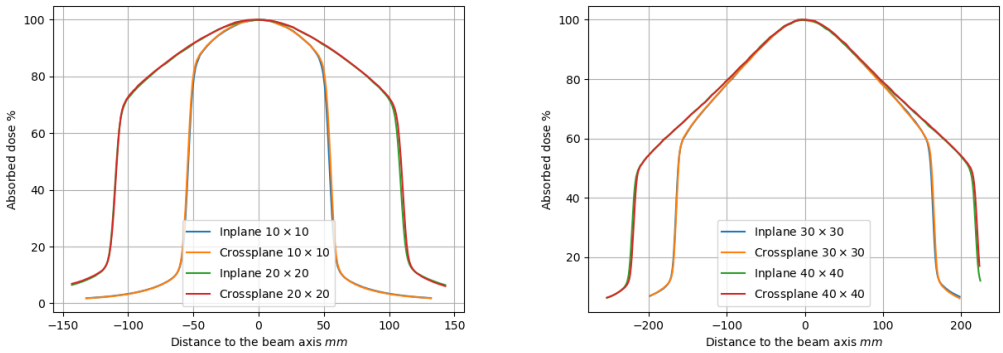

Figure 4.5: Profiles at 10 cm depth for FFF beam.

As seen in Figure 4.4 and 4.5, it is not relevant to calculate the slopes for fields smaller than 10×10 cm^2, as the small fields lies in the broad profile peak that is rather homogeneous. In particular, for squared fields of $3cm$ side the slope is larger than 1 (more for 10 MV FFF), and the two points for calculating the slope are on the profile shoulder, leading to a meaningless value [11].

Size $[cm^2]$	Symmetry (%)			
	5 cm depth		10 cm depth	
	Cross	In	Cross	In
10×10	0.09	0.10	0.08	0.09
20×20	0.21	0.28	0.21	0.21
30×30	0.30	0.39	0.29	0.30
40×40	0.37	0.50	0.37	0.37

Table 4.6: Symmetry for FFF profiles.

As Equation 2.11 establishes, the nearer to 0, the more symmetric is the profile, so the obtained symmetries are acceptable.

Size $[cm^2]$	Slope left		Slope right		Mean Slope	
	Cross	In	Cross	In	Cross	In
10×10	0.31	0.36	-0.33	-0.36	0.32	0.36
20×20	0.59	0.59	-0.58	-0.59	0.59	0.59
30×30	0.63	0.64	-0.65	-0.63	0.64	0.64
40×40	0.68	0.68	-0.68	-0.67	0.68	0.68

Table 4.7: Slopes for FFF profiles at 5 *cm* depth.

Size $[cm^2]$	Slope left		Slope right		Mean Slope	
	Cross	In	Cross	In	Cross	In
10×10	0.28	0.28	-0.27	-0.30	0.28	0.29
20×20	0.43	0.44	-0.44	-0.44	0.43	0.44
30×30	0.47	0.48	-0.47	-0.47	0.47	0.47
40×40	0.50	0.50	-0.49	-0.50	0.50	0.50

Table 4.8: Slopes for FFF profiles at 10 *cm* depth.

The obtained slope values obtained in [11] (Table IV) differ from the reported in tables 4.7 and 4.8. Nevertheless, the behaviour of the increasing slope with the field size and the decreasing value with depth is achieved in this work.

Chapter 5

Conclusions.

Abstract. *Los resultados obtenidos forman parte del estado de referencia inicial del acelerador, de forma que en los controles de calidad se comprobará que los parámetros medidos no varíen en relación los resultados que aquí se exponen.*

This obtained results (and the ones obtained for the different energies of the LINAC) will be now recorded as the initial reference status of the accelerator. Following the rules in [1], a regular quality control of all the parameters will be executed so that every patient who needs radiotherapy, can be safely treated and scheduled with the *Truebeam*.

The novelty of the new LINAC, the Flattening Filter Free beams, are recent in the clinical world. This means that the parameters which define these beams may change their definition in order to improve the quality of radiation therapy.

This work has approached me to the professional career which, since I started the physics degree, I wanted to do. By doing this final project I have re-ensured this dream. I have been lucky, because it was precisely this year when the new LINAC reached to the *CHUC*. I was able to see how it was being built, so I could see most of the elements which are inside the headboard and the acceleration structure (referenced in Figure 1.1).

References

[1] C. P. Molina and F. L. Valverde, *Control de calidad en aceleradores de electrones para uso médico*. Sociedad Española de Física Médica, 2009.

[2] M. Martins and T. Silva, "Electron accelerators: History, applications, and perspectives," *Radiation Physics and Chemistry*, vol. 95, pp. 78 – 85, 2014. Proceedings of the 12th International Symposium on Radiation Physics (ISRP 2012).

[3] J. M. de la Vega Fernández, *Caracterización y control de calidad de la energía de los haces de electrones empleados en radioterapia*. PhD thesis, Universidad de Granada, 2015.

[4] Ángel Franco García, "El acelerador lineal." http://www.sc.ehu.es/sbweb/fisica/elecmagnet/movimiento/lineal/lineal.htm.

[5] "About varian | varian medical systems." https://www.varian.com/about-varian.

[6] A. Fogliata, R. Garcia, T. Knöös, G. Nicolini, A. Clivio, E. Vanetti, C. Khamphan, and L. Cozzi, "Definition of parameters for quality assurance of flattening filter free (FFF) photon beams in radiation therapy," *Medical Physics*, vol. 39, pp. 6455–6464, Oct. 2012.

[7] J. M. Pedraza, *Aspectos físicos de la garantía de calidad en radioterapia: Protocolo de control de calidad IAEA-TECDOC-1151*. OIEA, 06 2005.

[8] M. Lind, *Characteristics of a Flattening Filter Free Photon Beam - Measurements and Monte Carlo Simulations*. PhD thesis, Lund University, 2008.

[9] G. Knoll, *Radiation Detection and Measurement*. Wiley, 2010.

[10] *Absorbed Dose Determination in External Beam Radiotherapy*. No. 398 in Technical Reports Series, Vienna: INTERNATIONAL ATOMIC ENERGY AGENCY, 2001.

[11] A. Fogliata, J. Fleckenstein, F. Schneider, M. Pachoud, S. Ghandour, H. Krauss, G. Reggiori, A. Stravato, F. Lohr, M. Scorsetti, and L. Cozzi, "Flattening filter free beams from TrueBeam and versa HD units: Evaluation of the parameters for quality assurance," *Medical Physics*, vol. 43, pp. 205–212, Dec. 2015.

Appendix A

Parts of a LINAC.

An explanation of figure 1.1 is given in this appendix.

- A: Modulator. It's main function is to supply a voltage pulse to the microwave generator.
- B: Microwave generator. The acceleration of the electrons has place due to the absorption of the transported energy by a high powered microwave. The microwave is produced by two types of devices: magnetron and klystron. The former is a creator of amplified microwaves; the latter is an amplifier, so it needs an oscillator pilot that would create a low intensity microwave which would be amplified by the device.
- C: Wave guide. From the generator, the microwave is led to the acceleration structure through a wave guide. This wave guide is separated from the acceleration structure by a window which isolates the transmittance and reduces the possible losses.
- D: Electron source and injector. It's main function is to supply the electrons to the acceleration structure. The source has a cathode which emits electrons due to a thermionic effect, which are focused and driven to an anode. The injector controls the amount and the energy of the electrons that go into the acceleration structure. This energy is around 150 keV. All the ensemble is united with the first acceleration cavity.
- E: Accelerator guide. This structure has the function of rising the energy of the injected electrons to the necessary value for each mode. It is formed by a set of cylindrical resonant metallic cavities. The

electrons are accelerated "in phase" with the oscillating electric field which is inside the cavities. The energy of the electronic package is raised progressively while it moves forward.

- F: Bending magnet. It has 3 main functions: it changes the beam direction to the patient, it selects the energy spectrum which would come out through the exit window and it focuses the radiation beam. To do these tasks, a combination of magnetic fields is used.

  We know from classic electromagnetism that an electron with velocity $\mathbf{v}$ inside a magnetic field $\mathbf{B}$ is subjected to a force given by:

  $$\mathbf{F} = e\mathbf{v} \times \mathbf{B} \tag{A.1}$$

  where e is the electron charge. The electron follows a round trajectory of radius R given by:

  $$R = \frac{m_e v}{eB} \tag{A.2}$$

  To build the bending magnet, achromatic deflection systems are used, so the dispersion effects due to energy differences of the electrons are minimised, and therefore in their trajectories. This keeps the beam aligned.

- G: Headboard. The headboard has 8 different parts: the output window, which ends at the exit of the bending magnet; the cart that locates the scattering layers or the target when the LINAC works with electron or photons, respectively; the set of secondary scattering layers, common to every way of function with electrons, which are in charge of scattering the electrons to the periphery, homogenising the beam; the homogenising filter, which is used because photons are distributed in such way that they yield more in the direction of the impact and decrease symmetrically to the periphery, a fact which needs to be corrected; the monitor cameras, which control the features of the beam (dose rate, total rate, symmetry...), and if any threshold is exceeded, the security systems of the LINAC are activated; the structure formed by two pairs of mobile collimators which delimit the size of the beam in transversal directions; the accessory mounting system, where the extra supplies needed to conform the beam are located; and the electron applier, which determines the size and shape of the radiation field in the patient's surface.

- H: Vacuum pump. It's function is to keep the high vacuum needed in the acceleration structure.

- I: Frequencies control system. The resonance frequency of the accelerator changes due to the variations in the geometric conditions (produced by temperature changes) or in the impedance of the guide (produced by the variation in the number of electrons injected). To keep the stationary conditions it is necessary to adapt the frequency constantly, so this is the function of this control system.

- J: Electric and safety systems. This systems are in charge of monitoring every feature of the LINAC. If the value of a parameter is over a certain threshold, the LINAC stops and a safety interlock is activated.

- K: Pressure diffuser. The gas used to fill the wave guide is SF_6. This system ensures that the pressure of the gas is appropriate.

- L: Refrigeration system. This system is in charge of keeping the temperature constant in the items (acceleration structure, microwave generator, the entry window, the bending magnet, the bending magnet exit window and the photon target). Without this system the temperature would increase to very high values.

- M: Control console. This is where technicians control the application of the treatments and verify the parameters of the LINAC [3].